The Trajectories of Line Current Differential Faults in the Alpha Plane

Gabriel Benmouyal
Schweitzer Engineering Laboratories, Inc.

Published in
Line Current Differential Protection: A Collection of Technical Papers Representing Modern Solutions, 2014

Previously published in
SEL *Journal of Reliable Power*, Volume 2, Number 3, September 2011

Originally presented at the
32nd Annual Western Protective Relay Conference, October 2005

The Trajectories of Line Current Differential Faults in the Alpha Plane

Gabriel Benmouyal, *Schweitzer Engineering Laboratories, Inc.*

***Abstract*—For a long time, the Alpha Plane has been a tool available to protection engineers to study line current differential characteristics and faults. The Alpha Plane constitutes a geometrical representation of the ratio of the two phase currents (or sequence currents) entering and leaving a transmission line in the complex plane. More recently, digital line current differential relays have been put into the market that have characteristics directly implemented into the Alpha Plane. A fault exists when the ratio locus gets outside a defined stability area. This paper studies the different trajectories of the current ratio depending upon contingency conditions: the type of element (phase or sequence), the line loading, the line length, the level of fault resistance, the level of current transformer (CT) saturation, if any, the presence of an open pole, or similar conditions.**

I. Introduction

Protection engineers are familiar with the concept of representing an impedance trajectory in the complex or R-X plane within the context of a distance-type transmission line protection scheme. They are less familiar with the concept of representing a current-ratio trajectory within the context of a transmission-line current differential protection scheme. The Alpha Plane was defined many decades ago for that very purpose.

The Alpha Plane is a geometrical representation of the ratio of the two phase currents (or sequence currents) phasors entering and leaving a transmission line in the complex plane. It has been, for a long time, a tool available to protection engineers to study line current differential characteristics and faults. It is also well established that any percentage differential characteristic can be mapped into the Alpha Plane so that both areas of stability and tripping can be determined as a function of the basic characteristic parameters.

More recently, digital line current differential relays have been put on the market the characteristics of which are directly implemented into the Alpha Plane. Basically, these relays compute the ratio of the phase (or sequence) currents entering and leaving the transmission line and determine whether the location of this ratio falls within a stability area directly embedded into the Alpha Plane. In order to accurately determine the limits of the stability area, it is necessary to study the trajectories of faults in the Alpha Plane and to ensure that these trajectories do not infringe into the stability area.

The trajectory of the current ratio corresponding to a particular fault will depend upon a number of factors, which could include:

- The nature of the current ratio: phase or sequence currents
- The line loading
- The line length
- The level of fault resistance
- The level of current transformer (CT) saturation, if any
- The presence of an open pole
- The presence of capacitive series compensation

The most complex trajectories will depend upon a combination of these factors. As an example, a long line with an open pole and a subsequent resistive fault will undergo a fault trajectory found in no other situation. Equally interesting, a series-compensated line will undergo a unique trajectory affected by the subsynchronous frequency present in the currents during the fault.

It is the purpose of this paper to review and study these different situations and to present basic rules for how to define line current differential characteristics in the Alpha Plane in order to optimize relay sensitivity, security, and reliability.

II. Review of Line Current Differential Phase and Sequence Elements Alpha Plane Characteristics

Reference [1] introduced the concept of a digital characteristic implemented into the current-ratio plane for line current differential elements. This is represented in Fig. 1. It consisted of computing the ratio of the remote current, IR, (phase or sequence current) over the local current, IL, and verifying that it lies inside the shown stability area.

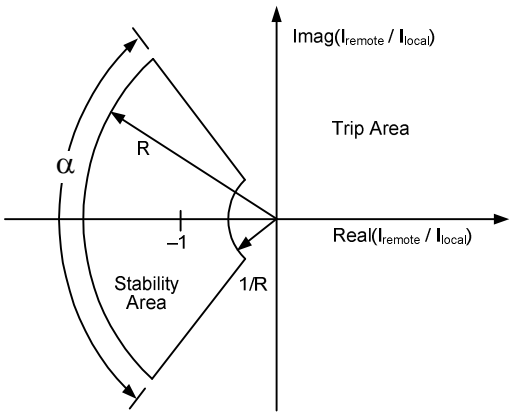

Fig. 1. Differential element characteristic embedded in the current-ratio plane

In a no-fault situation, the ratio would be close to the minus one point (–1,0). There are two settings for this characteristic, the radius, R, of the greater arc (typically between 5 and 10) and the angle alpha (typically between 160 and 210 degrees). This newly defined characteristic was an improvement with

respect to the so-called "rainbow" characteristic covered in [4] because of its total digital implementation and the additional control over the angle alpha (α) that was set to a fixed value of 180 degrees in the original concept. It will be shown later in this paper, how the additional control on the angle α can be useful in situations like CT saturation and series-compensated transmission lines.

How the ratio is performed is irrelevant when studying a characteristic performance. The local current on one side of a line becomes the remote current on the other side of the line and vice versa. Whether the results, therefore, are presented at one extremity of the line or the other is strictly equivalent.

III. Protection Scheme Based On Characteristics In the Alpha Plane

In the present study, it will be assumed that the line protection scheme, as shown in Fig. 2, is composed at each line extremity of 5 elements: three phase elements designated 87LA, 87LB, 87LC, one zero-sequence or ground element designated 87LG or 87L0, and one negative-sequence element designated 87L2.

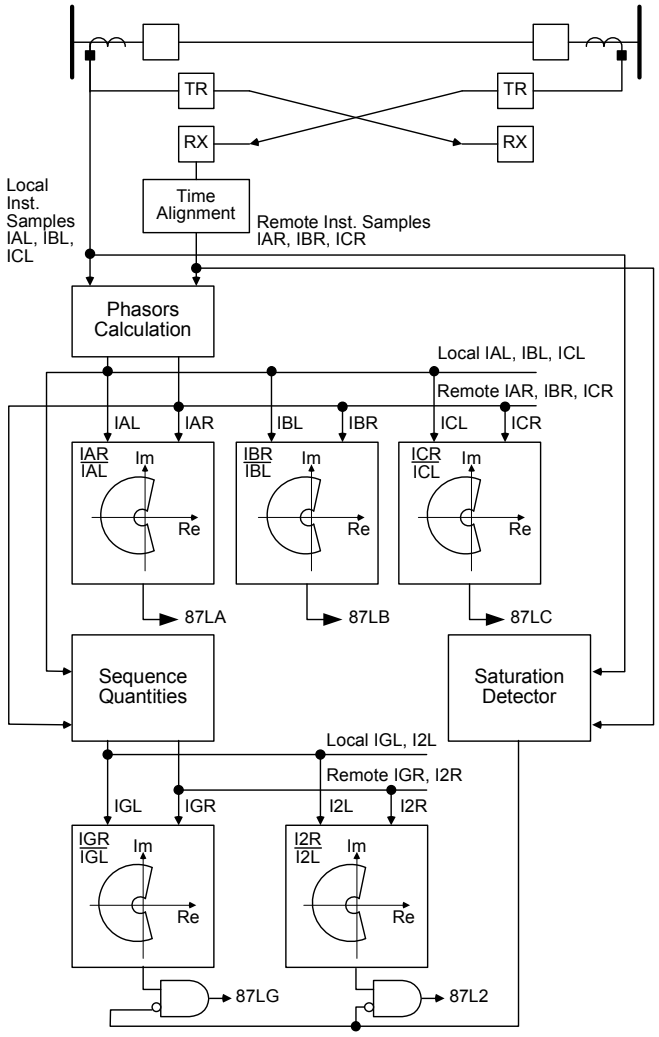

Fig. 2. Principle of line current differential protection scheme

A saturation detector supervises both the 87LG and 87L2 elements so that their operation is blocked if CT saturation is detected on any of the six phase currents involved. The rationale for and the details of this saturation detector are extensively covered in [2] and will be briefly revisited later in this paper.

IV. Trajectories of Faults for Short Line

For the purpose of this study, a line is considered to be short if it has negligible shunt capacitance.

A. Trajectories of Current Ratio in Phase Elements

Consider the elementary power network shown in Fig. 3. It consists of a single transmission line with two generators.

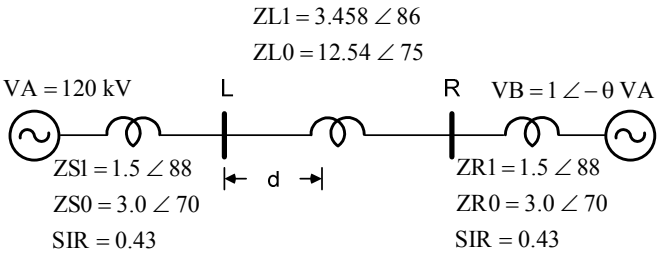

Fig. 3. 120 kV elementary network

The angle θ between the two sources determines the amount of line loading. Faults are applied at a distance, d, from the left bus. As is shown in Appendix A, the phase-A left bus current for a phase-A-to-ground fault is provided by:

$$IAL = C1\, I1F + C2\, I2F + C0\, I0F + I_{LD} \tag{1}$$

or:

$$IAL = (2\, C1 + C0)\, I1F + I_{LD} \tag{2}$$

In (1) and (2), C1 and C0 are the sequence network positive- and zero-sequence current distribution factors, I1F is the pure fault positive-sequence current at the fault, and I_{LD} is the load current.

Alternatively, the phase-A current at the right bus is provided by:

$$IAR = \left[2\,(1-C1) + (1-C0)\right] I1F - I_{LD} \tag{3}$$

Performing the ratio of the two phase-A currents at the extremities of the line results in:

$$\frac{IAR}{IAL} = \frac{\left[2\,(1-C1) + (1-C0)\right] I1F - I_{LD}}{(2\,C1 + C0)\, I1F + I_{LD}} = \frac{\left[2\,(1-C1) + (1-C0)\right] - \dfrac{I_{LD}}{I1F}}{(2\,C1 + C0) + \dfrac{I_{LD}}{I1F}} \tag{4}$$

Examination of (4) shows that the current ratio at the relay is dependent on the sequence current distribution factors and the ratio of the load current over the pure fault current at the fault location. The load current depends only upon the angle between the two sources and is equal to:

$$I_{LD} = \frac{\left(1 - e^{-j\theta}\right) VA}{ZS1 + ZL1 + ZR1} \tag{5}$$

The pure fault current depends upon the fault location, d; the current distribution factors and the fault resistance; as in:

$$I1F = \left[VA - ILD\left(ZS1 + d\ ZL1\right)\right] \div \left[\frac{2\left(ZS1 + d\ ZL1\right)\left(ZR1 + \left(1-d\right)ZL1\right)}{ZS1 + ZL1 + ZR1} + \frac{\left(ZS0 + d\ ZL0\right)\left(ZR0 + \left(1-d\right)ZL0\right)}{ZS0 + ZL0 + ZR0} + 3\ Rf\right] \tag{6}$$

Obviously, as the fault resistance increases, the pure fault current becomes smaller and smaller. Starting from (4), in a no-fault situation that is equivalent to a fault with infinite resistance, the pure fault current is equal to zero and the current ratio is simply equal to minus one, as in the next equation. Obviously the current ratio falls within the stability area in the Alpha Plane.

$$\frac{IAR}{IAL} = -1 \tag{7}$$

Also from (4), if the load current is equal to zero, the current ratio becomes independent from the pure fault current and, therefore, from the fault resistance. In this situation, the current ratio is dependent only on the sequence current distribution factors, as in:

$$\frac{IAR}{IAL} = \frac{\left[2\left(1-C1\right)+\left(1-C0\right)\right]}{\left(2\,C1+C0\right)} \tag{8}$$

Let us define the two constants a and b as:

$$\begin{aligned} a &= 2\,C1 + C0 \\ b &= 2\left(1-C1\right)+\left(1-C0\right) \end{aligned} \tag{9}$$

The phase-A current ratio can be expressed as a function of the load-to-pure-fault current ratio as:

$$\frac{IAR}{IAL} = \frac{b - \frac{I_{LD}}{I1F}}{a + \frac{I_{LD}}{I1F}} \tag{10}$$

The load-to-pure-fault current ratio can, in turn, be expressed as a function of phase-current ratio:

$$\frac{I_{LD}}{I1F} = \frac{b - a\frac{IAR}{IAL}}{1 + \frac{IAR}{IAL}} \tag{11}$$

Based on (11), if, for a particular network and a particular stability characteristic in the Alpha Plane, we plot the contour corresponding to the load-to-pure-fault ratio when we travel around the stability perimeter, we obtain a new perimeter that defines the limit of the element sensitivity as a function of the load-to-pure-fault current ratio.

As an example, for the elementary network of Fig. 3, for a fault at a distance, d, equal to 0 and 1 from the left bus and for a stability perimeter with radius 6 and angle $\alpha = 180°$, we obtain the load-to-pure-fault current ratio sensitivity perimeter shown in Fig. 4. If, for a particular network and a given fault, the load-to-pure-fault current ratio falls inside the sensitivity perimeters, the fault current ratio will fall outside the stability perimeter and it will be detected. If the load-to-pure-fault current ratio falls outside the sensitivity perimeter, the fault will not be detected. We verify that if the load is equal to zero, the load-to-pure-fault current ratio falls automatically inside the sensitivity perimeter and the fault is detected.

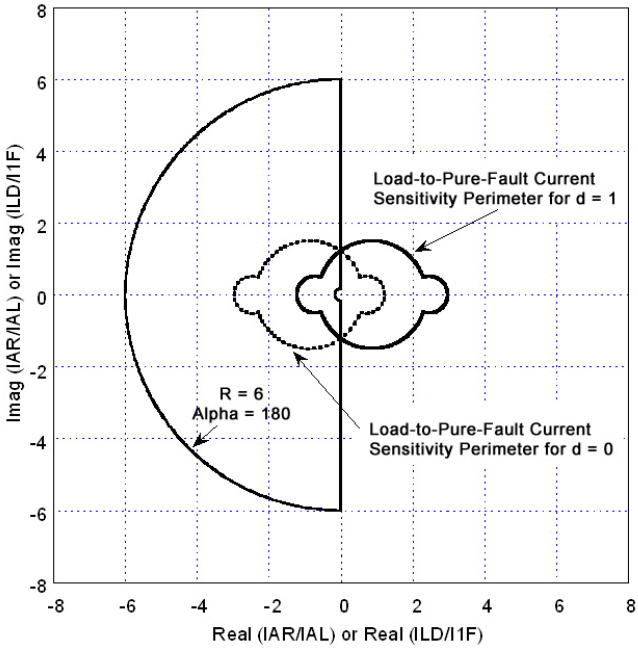

Fig. 4. Load-to-pure-fault current ratio sensitivity perimeter for phase-A-to-G faults

Looking at (6), there are two ways the pure fault current can be reduced so that the load-to-pure-fault current ratio will become larger to the point where the phase element will lose its sensitivity and will not detect a fault:

- Situation I: increase the value of the fault resistance. For a phase-to-ground fault, there is always a maximum value of fault resistance beyond which the phase element will become blind to a fault.
- Situation II: increase the value of the source impedances as would happen in a system where the system impedance ratio (SIR) is high at both extremities of the line. In such a situation, in order to supply the same load current, the load angle between the two sources will have to assume a higher value.

Fig. 5 illustrates Situation I by exhibiting the trajectories of the phase-A current ratio for the elementary network of Fig. 3 when a phase-A-to-ground fault is applied at three different locations on the line. In all cases, the load angle between the two sources is 5 degrees. For each of the three fault locations, the fault resistance is varied from zero to 100 ohms primary, with increments of 1 ohm. Obviously, as the fault resistance increases, the ratio of the load current over the pure fault current becomes high enough that the trajectory enters the stability area so that the phase element becomes blind to the fault.

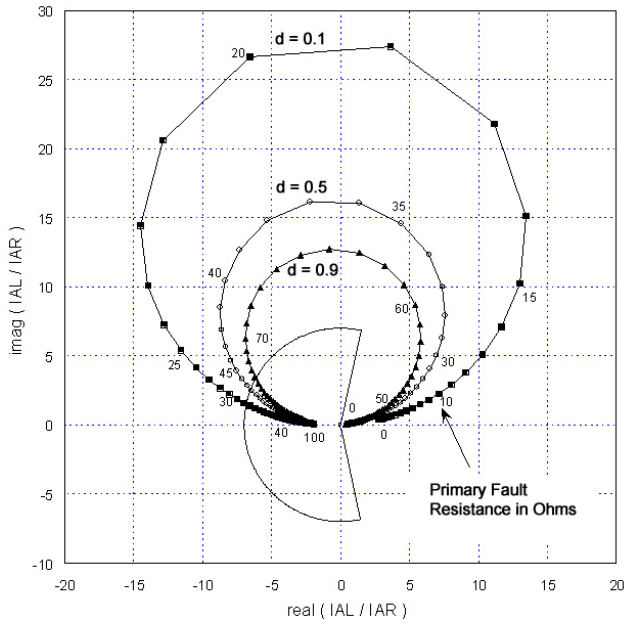

Fig. 5. 87LA trajectories for a phase-A-to-G fault at three locations and variable fault resistance

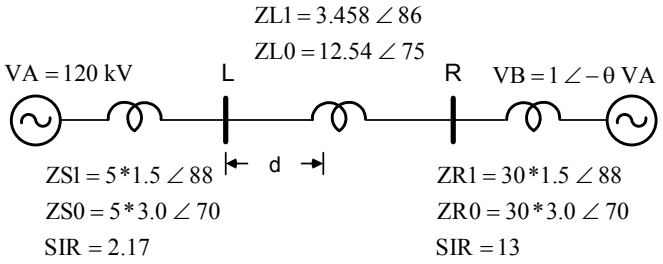

Fig. 6. 120 kV elementary network with higher SIR

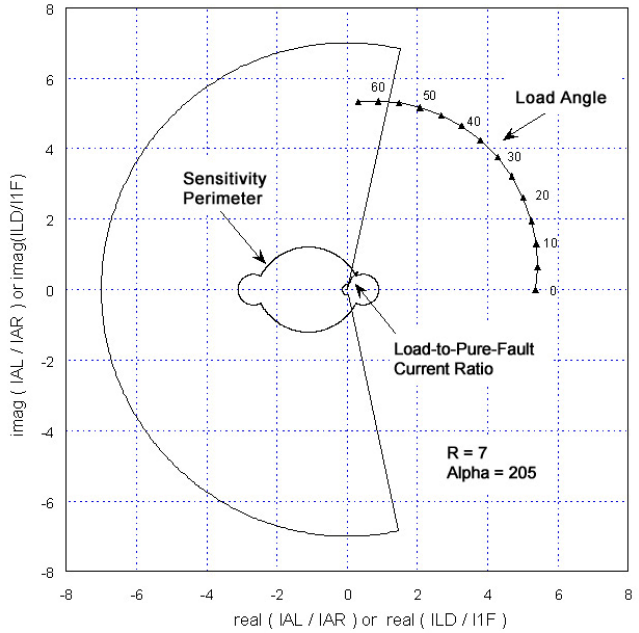

Fig. 7. 87LA trajectories for a phase-A-to-G fault at d = 0.33 with varying load angle

To illustrate Situation II, we multiply the source impedances of the network in Fig. 3 by five on the left side (SIR of 2.17) and by 30 on the right side (SIR of 13), as represented in Fig. 6. To keep the same amount of load current, we must then increase the load angle between the two sources to keep the load angle between the two sources. Fig. 7 shows the location of the current ratio for a phase-A-to-ground fault at location d = 0.33 when the load angle assumes values of 0 to 65 degrees with steps of 5 degrees.

On the same figure, the corresponding characteristic sensitivity perimeter has been drawn. This figure also shows the trajectory of the load-over-pure-fault current ratio. As indicated by the trajectory entering the stability area, there is a value of load angle of about 55 degrees when the load-over-pure-fault current ratio locus leaves the perimeter of sensitivity, indicating that the element has become blind to the fault.

B. Trajectories of Sequence Elements

From Appendix A, the ratio of the zero-sequence currents at the extremities of the line is provided as:

$$\frac{I0R}{I0L} = \frac{(1-C0)\,I0F}{C0\;\;I0F} = \frac{(1-C0)}{C0} = \frac{d\;ZL0 + ZS0}{(1-d)\;ZL0 + ZR0} \quad (12)$$

In the same fashion, the ratio of the negative-sequence current at the two extremities of the line is:

$$\frac{I2R}{I2L} = \frac{(1-C1)\,I1F}{C1\;\;I1F} = \frac{(1-C1)}{C1} = \frac{d\;ZL1 + ZS1}{(1-d)\;ZL1 + ZR1} \quad (13)$$

Looking at (12) and (13), we see that the current ratios of the zero- and negative-sequence currents are totally independent from the load current and angle, the pure fault current, and, consequently, the fault resistance. The ratio depends only on the current distribution factors and, consequently, upon the fault location d. If the two sources had the same impedance and the fault location was the middle of the line, the current ratio of both 87LG and 87L2 elements would be the points (1,0) in (x,y) coordinates in the trip area.

It could be said that the 87LG and 87L2 elements have a theoretical infinite sensitivity to resistive ground faults. However, this could only be stated for perfectly transposed networks and perfect CTs. In reality, a limit to this sensitivity would be set by a minimum sequence (negative or zero) differential pickup current in order to take into account the natural unbalances in the network, the CT errors, and so forth.

As an example, Fig. 8 represents the locus of the negative-sequence current ratio when a phase-A-to-ground fault is applied at locations from 0 to 1, per unit of line length for the elementary network of Fig. 3. Note that this current ratio trajectory is totally independent from the fault resistance and the load angle. Because all the network impedances are inductive, the negative-sequence currents ratio is located close to the horizontal axis on the right-hand side half-plane that belongs to the trip area. Fig. 9 represents the same locus for the zero-sequence ratio under the same conditions.

C. Phase Element With Removal of the Load Current

The load current is the current that exists on the line prior to the fault. Referring back to (4), subtracting the load current

from the fault current prior to computing the current ratio would yield:

$$\frac{IAR - IAR_{preflt}}{IAL - IAL_{preflt}} = \frac{\left[2\left(1-C1\right)+\left(1-C0\right)I1F - I_{LD} + I_{LD}\right]}{\left(2\,C1+C0\right)I1F + I_{LD} - I_{LD}} = \frac{2\left(1-C1\right)+\left(1-C0\right)}{2\,C1+C0} \quad (14)$$

Equation (14) indicates that the phase current ratio of an 87LA element where the load current has been removed from the fault current is now dependent only on the sequence current distribution factors and, therefore, the network impedances. This element would have the same insensitivity as an 87LG or 87L2 element with respect to resistive faults and load angle.

Fig. 10 represents the trajectory of the 87LA element when the prefault current is removed and when a phase-A-to-ground fault is applied from distance 0 to 1, with a fault resistance of 100 ohms. Obviously, the element has become insensitive to the fault resistance.

In the scheme of Fig. 2, it is obvious that there is no necessity to remove the load current from the phase elements because the high level of sensitivity is already guaranteed by the two sequence elements, 87LG and 87L2.

V. Trajectories of Faults for a Short Line With an Open Pole

A. Case of a Single-Phase-A-to-Ground Fault With Phase-B Open

Consider the elementary network of Fig. 3 and assume that single-pole tripping has been instituted on the line protection scheme. Let us further assume, as an example, that phase-B is open and that a subsequent phase-A-to-ground fault occurs. We want to investigate the sensitivity of the phase and sequence elements in this new situation.

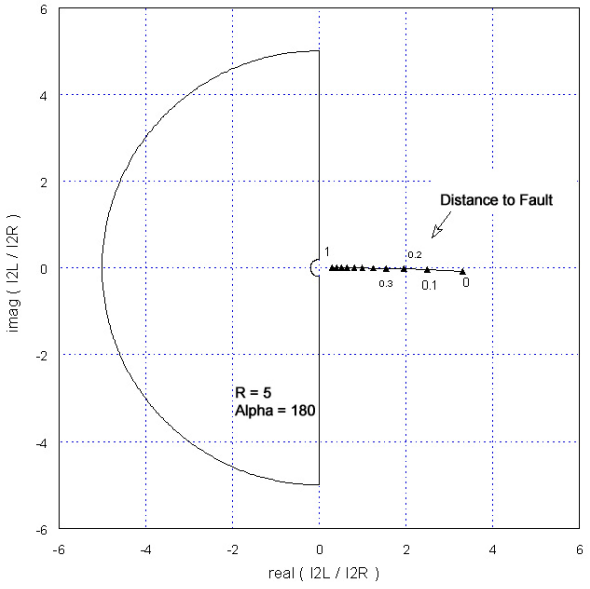

Fig. 8. 87L2 trajectories for a phase-A-to-G fault at different locations

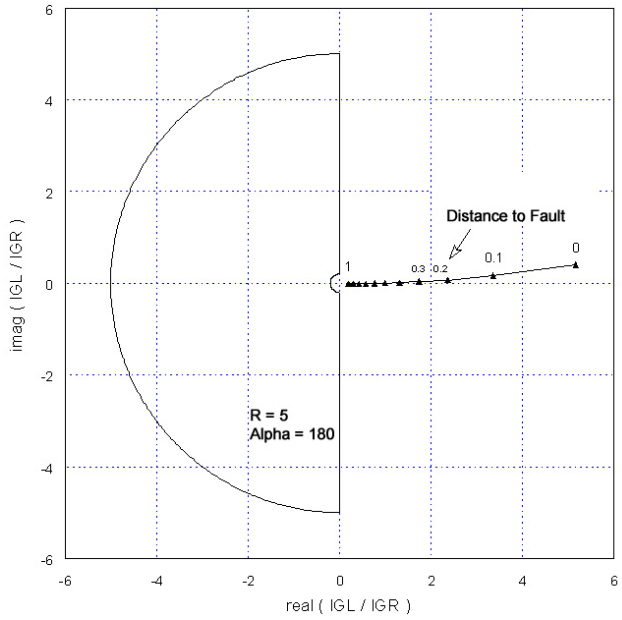

Fig. 9. 87LG trajectories for a phase-A-to-ground fault at different locations

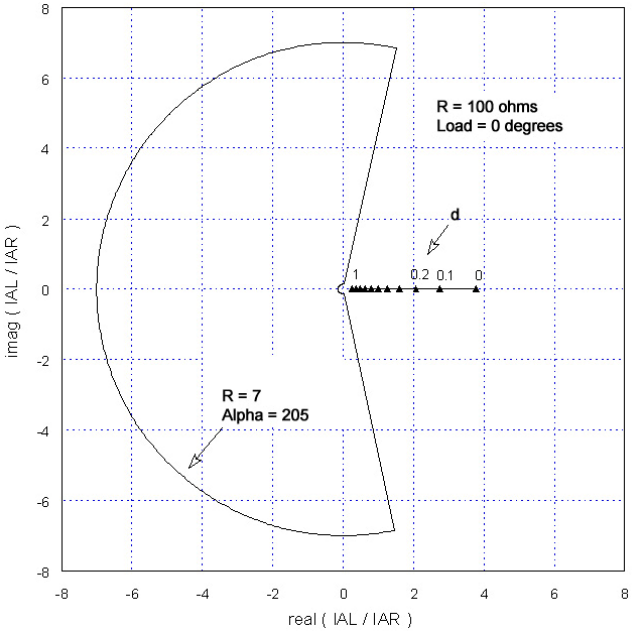

Fig. 10. 87LA element trajectories for a phase-A-to-G fault at different locations with no load and fault resistance of 100 ohms

A thorough analysis of a phase-A-to-ground fault during a phase-B open is presented in Appendix B, with the computation of phase-A and sequence currents during the fault using the proper sequence network.

The current ratio of the 87LA element is provided as:

$$\frac{IAR}{IAL} = \frac{IAR_{preflt} + \left(2 + \frac{p + 2\,q - 0.5\left(m_1 + 2\,n_1\right)}{m + 2\,n} + \frac{3\,m_1}{2\,m}\right)IF}{IAL_{preflt} - \frac{3}{2}\left(\frac{m_1 + 2\,n_1}{m + 2\,n} + \frac{m_1}{m}\right)IF} \quad (15)$$

where the current through the fault IF is given as a function [see (60) in Appendix B] of the distance to the fault d, the

network impedances, the source voltages, and the fault resistance Rf, as in:

$$IF = \text{func}\left(d, ZS1, ZL1, ZR1, ZS0, ZL0, ZR0, R, VA, VB\right) \quad (16)$$

Variables p, q, m, n, m_1, n_1 are defined in (52) in Appendix B.

As in the case of the three-pole trip application, (15) indicates that the trajectory of the 87LA element in a single-pole trip application will be dependent upon the distance to the fault, the network impedances, the source voltages, and the fault resistance R_f.

For the elementary network of Fig. 3, the plot in Fig. 11 shows the trajectory in the Alpha Plane of the current ratio for the 87LA when a phase-A-to-ground fault is applied at 33 percent of the line length and phase-B is open. The primary fault resistance is varied from 0 to 100 ohms.

The current ratio for the 87L2 element is provided by:

$$\frac{I2L}{I2R} = \frac{\dfrac{-a\,\Delta V\,n}{m\left(m+2\,n\right)} + \left(\dfrac{a^2}{2}\dfrac{\left(m_1+2\,n_1\right)}{m+2\,n} + \dfrac{m_1\left(1-a\right)}{2\,m}\right)IF}{\dfrac{a\,\Delta V\,n}{m\left(m+2\,n\right)} + \left(1-\dfrac{a^2}{2}\dfrac{m_1+2\,n_1}{m+2\,n} + \dfrac{m_1\left(1-a\right)}{2\,m}\right)IF} \quad (17)$$

The sequence ratio for the 87L0 element is:

$$\frac{I0L}{I0R} = \frac{\dfrac{-a^2\,\Delta V}{m+2\,n} - \dfrac{m_1+2\,n_1}{m+2\,n}IF}{\dfrac{a^2\,\Delta V}{m+2\,n} + \dfrac{p+2\,q}{m+2\,n}IF} \quad (18)$$

Examining (17) and (18), we can see that, contrary to the three-pole tripping application, the current ratio in the 87L2 and 87LG elements is no longer independent from the fault resistance R_f, the source voltages, and the current at the fault IF.

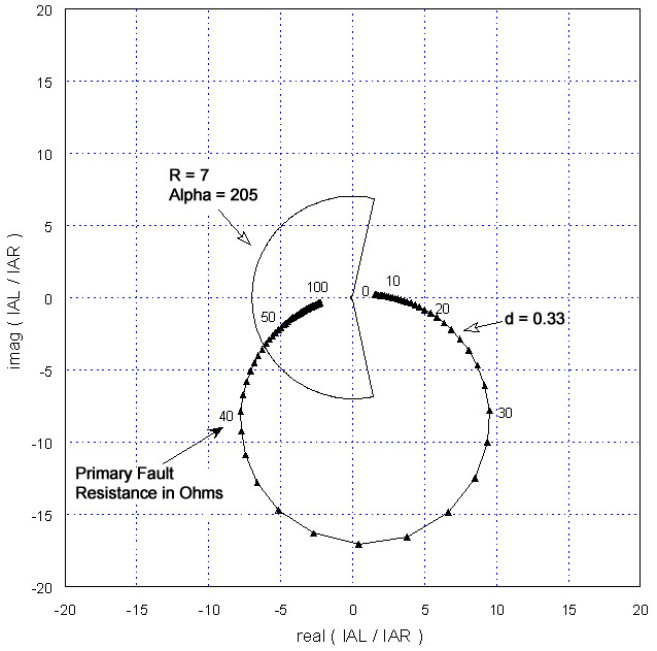

Fig. 11. 87LA element trajectory during a phase-B open with a phase-A-to-G fault with varying fault resistance

Fig. 12 and Fig. 13 show the trajectory of the current ratio for the 87L2 and 87LG elements under the same conditions as the phase element. Examining the plots in Fig. 12 and Fig. 13, we can see that, contrary to the three-pole trip application, the 87L2 and 87LG elements lose their sensitivity in a single-pole trip application with respect to resistive faults. We could even claim that the sequence elements are no more sensitive than the phase element itself.

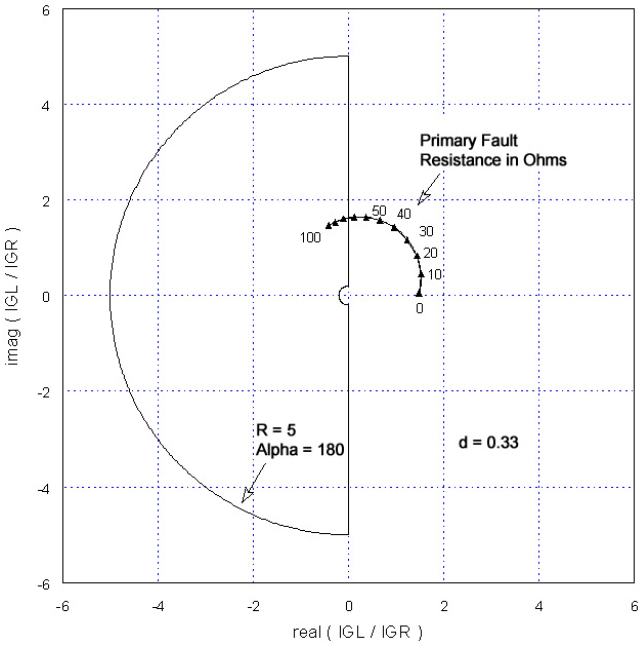

Fig. 12. 87LG element trajectory during a phase-B open with a phase-A-to-G fault with varying fault resistance

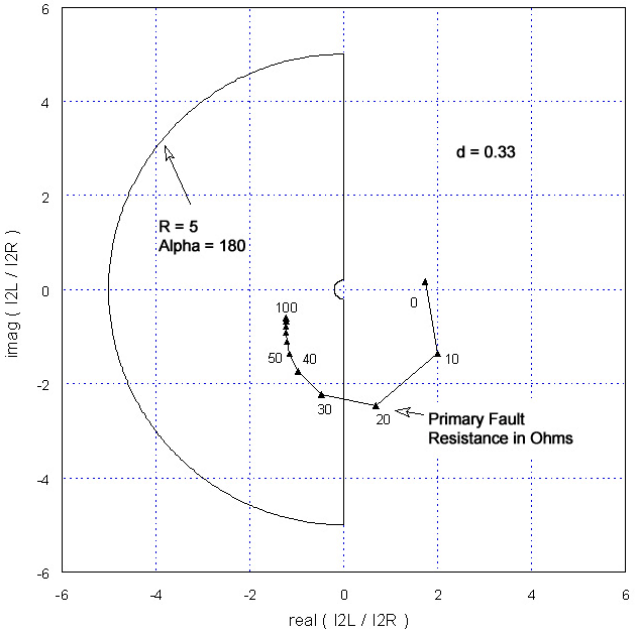

Fig. 13. 87L2 element trajectory during a phase-B open with a phase-A-to-G fault with varying fault resistance

B. Removal of the Prefault Current in the Sequence Elements During an Open Pole

As shown in Appendix B, during an open pole, there are negative- and zero-sequence currents flowing into the line.

The 87L2 and 87LG elements will process these sequence currents as if they belong to an external fault and, consequently, will not pick up. If during an open pole we systematically remove the prefault sequence currents when computing the current ratio in the 87L2 and 87LG elements, we end up with:

$$\frac{I0L - I0L_{preflt}}{I0R - I0R_{preflt}} = \frac{-\frac{m_1 + 2n_1}{m + 2n} IF}{\frac{p + 2q}{m + 2n} IF} = \frac{-(m_1 + 2n_1)}{p + 2q} \quad (19)$$

$$\frac{I2L - I2L_{preflt}}{I2R - I2R_{preflt}} = \frac{\frac{a^2}{2}\frac{m_1 + 2n_1}{m + 2n} - \frac{m_1 (1 - a)}{2m}}{1 - \frac{a^2}{2}\frac{m_1 + 2n_1}{m + 2n} + \frac{m_1 (1 - a)}{2m}} \quad (20)$$

Examining (19) and (20), we can see that the removal of the prefault current for a fault occurring during an open-pole situation has rendered the element independent from the current flowing into the fault, and consequently, independent from the fault resistance. The sequence elements can be made once again to have virtually infinite sensitivity to resistive faults.

Fig. 14 shows the locations of the 87L2 element current ratio for a phase-A-to-ground fault at 33 percent of line length during a phase-B pole-open situation with a primary fault resistance of 50 ohms for the elementary network of Fig. 3. Fig. 14 shows two loci: one locus with the prefault currents kept in the current ratio and a second locus with the prefault currents removed from the current ratio. The obvious consequence of the prefault currents removal is to restore the 87L2 element sensitive by moving the current ratio locus from the stability to the trip area.

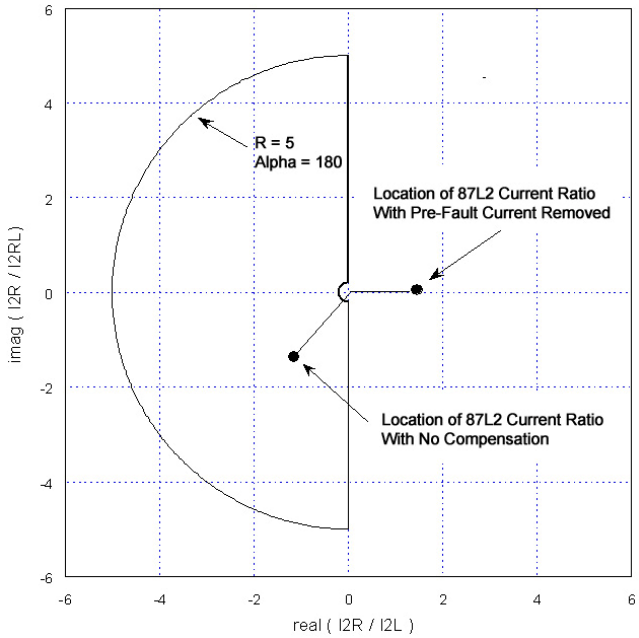

Fig. 14. 87L2 element current ratio loci during a phase-B open with a phase-A-to-G fault with prefault current present and removed

C. Removal of the Prefault Current in the Phase Elements During an Open Pole

The prefault current can be removed from the phase elements as well. For the 87LA element, the resulting current ratio is represented in (21). Obviously, the current ratio has become dependent only upon the fault location d and the fixed network impedances. The compensated 87LA element will be able to detect resistive faults with the same sensitivity as the sequence elements do.

$$\frac{IAR - IAR_{preflt}}{IAL - IAL_{preflt}} = \frac{\left(2 + \frac{p + 2q - 0.5(m_1 + 2n_1)}{m + 2n} + \frac{3m_1}{2m}\right)}{-\frac{3}{2}\left(\frac{m_1 + 2n_1}{m + 2n} + \frac{m_1}{m}\right)} \quad (21)$$

At this stage, is there justification for removing the prefault current from the phase elements during an open pole? For the sake of implementation simplicity, it is recommended that the prefault current from the two sequence elements, 87LG and 87L2, be removed only during an open-pole situation. There is no need to remove them from the phase elements, since 87LG and 87L2 will provide the necessary sensitivity.

VI. Trajectories of Faults for Long Lines

For the purpose of this study, a long line is defined as one having significant shunt capacitance.

A. Long Lines Impact on Phase Differential Elements

The most important impact of long lines on phase differential elements is the presence of significant shunt capacitance. As a consequence, important current will be drawn by this shunt capacitor at the relay location. In a no-load situation (no current flowing into the line), a phase differential element will see the current ratio caused by the shunt capacitance at both extremities of the line fall into the trip area because the current-ratio phase angle will be close to zero. To prevent a misoperation caused by the shunt current, it is necessary to impose a threshold that does not allow the phase differential element to operate unless the phase current is greater than the shunt current.

B. Long Lines Impact on Sequence Differential Elements

In three-pole tripping applications, the impact of shunt capacitances on the 87L2 or 87LG elements can be neglected because the shunt currents corresponding to the three phases are balanced. Consequently, they disappear when the local zero- or negative-sequence currents are determined.

The situation is different in single-pole tripping applications. During a pole-open situation, the local negative- or zero-sequence current caused by the shunt capacitances will not be zero, but will be equal in magnitude to one third of the original phase current caused by the shunt capacitance. In an open-pole situation, as applied for the phase element in three-pole-tripping situations, a threshold has to be imposed on the local sequence currents before the sequence element is allowed to operate.

C. Pole-Open Sequence Elements Compensation for Long Lines

The principle described for the compensation of sequence elements during single-pole tripping applications is still valid for long lines. The only difference is that the prefault current will now have two components: the combination of the local sequence current caused by the shunt capacitance plus the sequence current caused specifically by the pole-open situation [see (54) to (56) in Appendix B].

Consider the 500 kV long line of Fig. 15 and a resistive phase-A-to-ground fault occurring at 33 percent of the line length during a phase-B open condition. The primary fault resistance is 150 ohms. None of the 87LA or the sequence elements, 87LG and 87L2, will see the fault because the fault resistance will keep the different current ratios inside the respective stability area. When compensation by removal of the prefault current is applied, both the 87L2 and the 87LG elements will detect the fault.

Fig. 16 represents the 87L2 element trajectory without any compensation. Obviously, the trajectory remains confined inside the stability area. Fig. 17 represents the same element trajectory with removal of the prefault current. The element detects the fault under the new conditions.

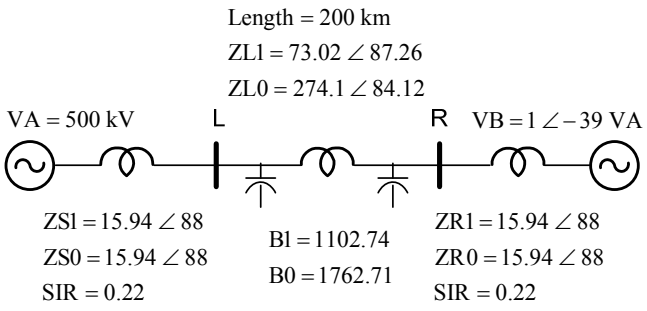

Fig. 15. 200 km 500 kV long line model

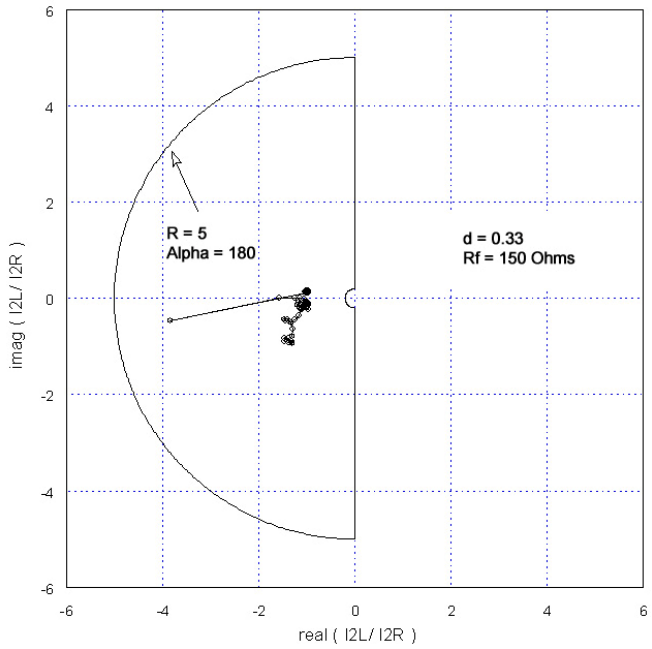

Fig. 16. 87L2 element current ratio loci during a phase-B open phase-A-to-G fault on a long line with fault resistance of 150 ohms with no compensation

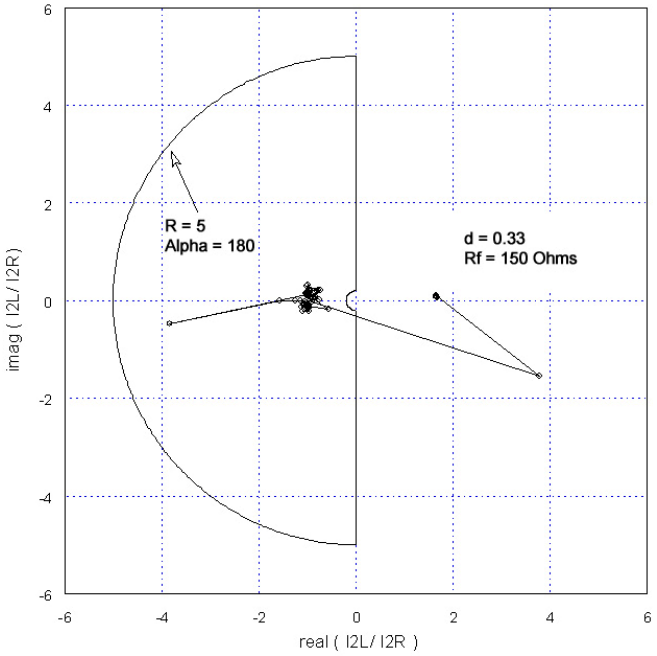

Fig. 17. 87L2 element current ratio loci during a phase-B open phase-A-to-G fault on a long line with fault resistance of 150 ohms with prefault current compensation

In this example, the compensation has been effective because the angle between the two sources has been set to 39 degrees and is an indication of a high loading level. Had the load not been so high, the sequence elements would have seen the fault even without any compensation. This result is consistent with the study of the impact of the load on short lines presented previously.

D. Trajectories of Faults With Series Compensation

1) Nature of Subsynchronous Resonance

The main impact of series-compensated lines on differential elements will be the presence of an additional frequency component in the currents caused by the presence of a well-known phenomenon called subfrequency resonance. This subsynchronous resonance typically occurs between 5 and 20 Hz. It can be apprehended by looking at Fig. 18, which represents a simplified model of a series-compensated line together with a shunt inductance. This circuit will exhibit a pole at the frequency f_0 equal to:

$$f_0 = \frac{1}{2\pi\sqrt{(L_s + L_p)C_s}} \tag{22}$$

Since the line inductance, L_s, is far smaller than the shunt inductance, L_p, the resonance will finally be determined by the series capacitance and the shunt inductance as in:

$$f_0 = \frac{1}{2\pi\sqrt{L_p C_s}} \tag{23}$$

This subsynchronous component will pervade the phase currents and is very difficult to remove by filtering, given the low value of the frequency component (low-pass filtering will impose delays much larger than the required protection response time).

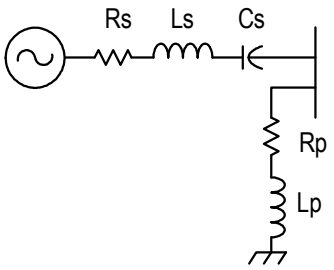

Fig. 18. Simplified representation of series and shunt compensation

E. Impact of Subsynchronous Component on Differential Element Current Ratio

To understand the impact of the subsynchronous component of the trajectory of the current ratio of the differential element, a phase-A-B-to-G fault has been simulated on the series-compensated network represented in Fig. 19.

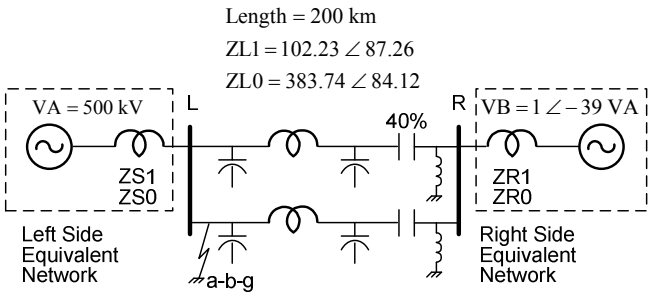

Fig. 19. Series-compensated network

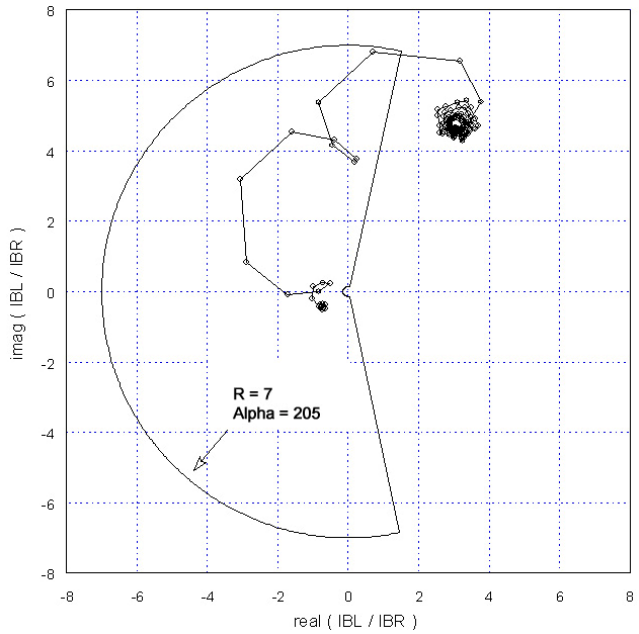

Fig. 20. Trajectory of 87LB for series-compensated line A-B-G fault

Fig. 20 represents the trajectory of the 87LB element. As you can see, the presence of the subfrequency component will cause the locus of the current ratio to oscillate around the final current ratio. The final location of the current ratio is close to the stability area because of the high level of loading on the line. A situation could develop with higher loading and greater oscillations where the trajectory during the fault will infringe on the stability area and the element will momentarily not detect the fault. Pulling the angle alpha back to a lower value can mitigate this situation.

Fig. 21 represents the trajectory of the 87L2 element during the fault. As explained previously, the effect of the sequence element is to remove the loading effect present on the phase element. Whereas the phase element could momentarily infringe on the stability area, the sequence element will perform a more secure trip even though its trajectory will undergo an equivalent oscillation because of the subsynchronous component.

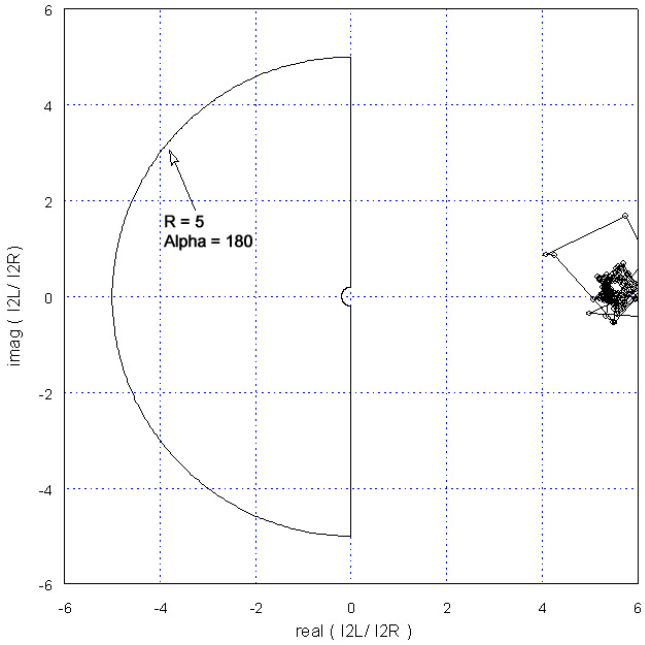

Fig. 21. Trajectory of 87L2 for series-compensated line A-B-G fault

VII. The Impact of External Faults With Single CT Saturation in the Alpha Plane

A. The Concept of a Saturated Current Phasor

The concept of the saturated current phasor, introduced in [2], allows transforming the essentially nonlinear CT saturation phenomenon into a linear problem. In digital relays where phasors are computed through a filtering process, the phasor of a saturated current can be defined as a linear transformation of the nonsaturated current phasor. This transformation involves a reduction in the magnitude, accompanied by a positive rotation of the phase angle.

The concept of a saturated current phasor as a linear transformation on the true phasor allows for taking into account saturation in relays characteristic equations that model numerical relays performance in steady state.

As an example, consider a fault of 20,000 A with an X/R ratio of 11.31 when the current is processed through a CT with the following characteristics:

ANSI voltage: 400 V
Turn ratio: 240
Burden: 2 ohms (purely resistive)

Fig. 22 shows the corresponding saturated secondary current together with the true current. This figure also shows the magnitudes of both currents as would be acquired by a numerical Cosine filtering system. Note that a full-cycle Fourier filter would exhibit similar results. Obviously, during the saturation interval, the acquired current magnitude is falling short of the true value.

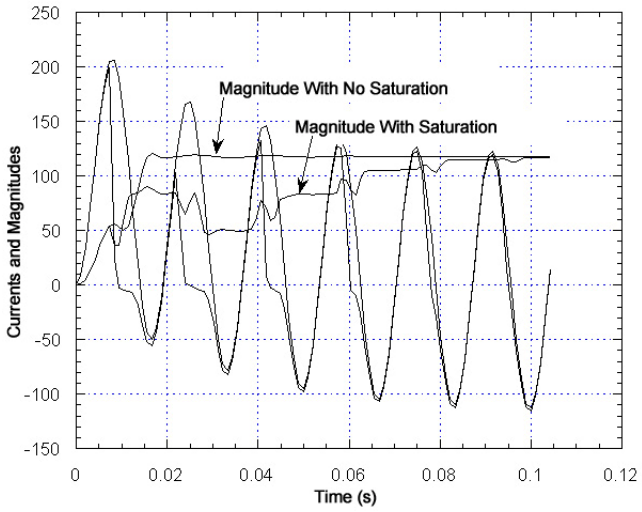

Fig. 22. CT saturation effect on a current phasor magnitude

Fig. 23 shows the ratio of the saturated current phasor magnitude over the true current phasor magnitude, as a Cosine filter filtering system would acquire them. Fig. 24 shows the phase advance of the saturated current phasor with respect to the nonsaturated current phasor and exhibits a maximum phase angle advance of 57 degrees.

Fig. 23 exhibits a minimum ratio of approximately 0.4.

Obviously, the impact of saturation on a current phasor is a transient phenomenon. The parameters of this transformation will vary with time until the magnitude reduction becomes one and the phase angle advance becomes zero when the saturation has vanished. However, a saturation level can be defined by the minimum magnitudes ratio and the maximum phase angle advance reached during the time the saturation takes place.

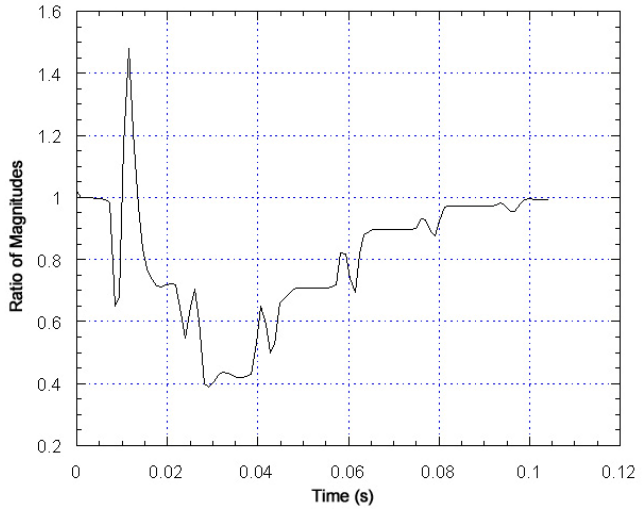

Fig. 23. Ratio of magnitudes of saturated over true current phasors

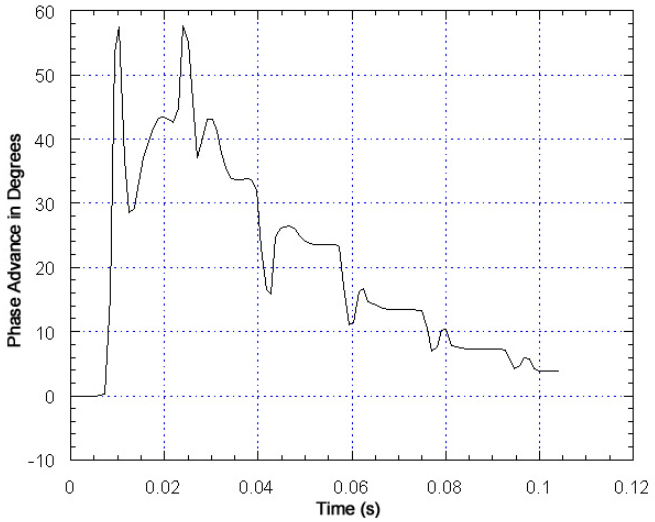

Fig. 24. Phase advance of saturated over true current phasor

Reference [2] proposes four levels of saturation as convenient definitions from low to extreme saturation. Assuming a true current phasor IA, the limits of the transformation to be applied to the true phasor to get the saturated current phasor, IA_sat, are defined in Table I for the four defined levels of saturation.

TABLE I
PHASOR TRANSFORMATION AS A FUNCTION OF SATURATION LEVEL

Saturation Level	Transformation
Low Saturation	IA_sat = (1–0.9) ∠ (0–10)° IA
Moderate Saturation	IA_sat = (0.9–0.5) ∠ (10–45)° IA
High Saturation	IA_sat = (0.5–0.2) ∠ (45–85)° IA
Extreme Saturation	IA_sat = (<0.2) ∠ (>85)° IA

When a CT saturates, the saturation level then will be defined as the one for which the minimum magnitude ratio found in the transient state does not get below the ratio defined for the particular saturation level. Alternatively, the maximum phase advance found in the transient state should not get above the phase advance defined for the same saturation level.

B. Performance of Phase Elements During External Faults With Single CT Saturation

For a numerical line current differential relay, the impact of a single CT saturation during an external fault on a phase current differential element (87LA, 87LB, or 87LC) is easily understood if the concept of the saturated current phasor is being used. Consider the same elementary network as before (Fig. 3) and assume a phase-B-to-ground fault occurs external to the line, as shown in Fig. 27. In the situation where there is no saturation, the location of any of the three phase current ratios IR/IL will be inside the stability area close to the point (–1,0). If saturation is present on one side of the line, the magnitude of the saturated current phasor will be reduced and it will undergo a rotation in proportion to the saturation level that could go beyond 90 degrees. As a consequence of the transformation imposed on the saturated current phasor, the

magnitude of the current ratio, during the time interval the saturation occurs, will depart from the stable position [close to (–1,0)] and take values that could go up to 0.1 (or 10, depending how the ratio is performed) for cases of high saturation and beyond for extreme situations. Alternatively, the current-ratio phase angle will depart from the stable position around 180 degrees and will undergo a rotation that will bring it to values close to ±90 degrees for high saturation levels and beyond for extreme saturation cases.

With the present characteristic implemented in the Alpha Plane, the user has two settings to cope with the expected level of saturation: the greater arc radius R and the angle alpha. As an example, a radius R between 8 and 10 and an angle between 180 and 210 will sustain high-to-extreme levels of saturation, as defined in Table I.

Fig. 28 shows the trajectory of the phase-B current ratio when the fault occurs and the right-hand side CT undergoes saturation. Note that the Alpha Plane characteristic will handle nicely the CT saturation. Also note that without saturation, the element trajectory should be around the point (–1,0).

C. Impact of a Distorted Phase Current on the Corresponding I0 or I2 Phasor

During an external ground fault, the zero- and negative-sequence currents measured at both extremities of a transmission line will be opposed in phase, as shown in Fig. 25. When the corresponding sequence differential current is computed, the result will be close to zero and the corresponding current-ratio plane elements 87L0 and 87L2 will not operate.

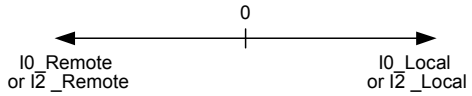

Fig. 25. Sequence currents during an external fault

During an external fault, the faulted phase CT could saturate. What is, then, the impact of a saturated CT on both sequence elements? The problem is to find the transformation on a sequence phasor (negative- or zero-sequence) that is a function of the saturated current phasor. This problem has been thoroughly analyzed in [2] and will be briefly reviewed here.

Assume that any type of external fault could occur, but that only the phase-A CT would saturate. Define two vectors, IS0 and IS2, as:

$$IS0 = IB + IC \tag{24}$$

and:

$$IS2 = a^2 IB + a\,IC \tag{25}$$

so that from (24) and (25), we have:

$$3I0 = IA + IS0 \tag{26}$$

$$3I2 = IA + IS2 \tag{27}$$

Obviously, IS0 and IS2 are the two vectors added to the phasor IA in order to obtain 3I0 and 3I2. Equations (26) and (27) are general by definition and could apply to any type of external fault. In the rest of the text, IS will represent interchangeably IS0 or IS2.

IA is defined as a unit phasor, and in Fig. 26, IS is represented with a phase-angle lag of approximately 120 degrees with respect to faulted phasor IA. By adding IA to IS0 or IS2, we obtain the local zero- or negative-sequence phasor I0 or I2. Assume that the phase-A current undergoes saturation and is subjected to a reduction in magnitude to 0.4 and a phase advance of 60 degrees. The corresponding saturated phasor is then IA_sat. The new zero- and negative-sequence phasors resulting from the saturation of phase-A are shown as I0_sat or I2_sat. For the example shown, we can see that I0_sat or I2_sat undergoes a rotation of practically 180 degrees with respect to the original position of I0 or I2 when the original rotation imposed by the saturation on IA was only 60 degrees.

This simple example has shown that for any type of external fault, it is possible to find locations of IS (IS0 or IS2) with respect to IA that will make the corresponding element 87LG or 87L2 unstable during a moderate saturation of the phase-A current. This example demonstrates that the possibility of a negative- or zero-sequence phasor undergoing a rotation of 180 degrees for a moderate saturation of the phase-A current makes it impossible to stabilize a sequence element when saturation occurs. This is true whether we use a characteristic in the Alpha Plane or a conventional dual-slope characteristic to implement the sequence element.

For this reason, [2] has introduced the concept of a saturation detector that blocks the sequence elements (87LG and 87L2) when saturation is detected on any of the six processed phase currents. This justifies the blocking of the sequence elements as represented in the protection scheme of Fig. 2.

Fig. 29 represents the 87LG elements current ratio for the same phase-B-to-ground fault. Obviously, the element is completely unstable because of the saturation, even though radius R has been set to 7 and the angle alpha is equal to 215 degrees. Although it has been possible to stabilize the phase-B element, this is not the case with the 87LG element, which is why it is simply blocked to prevent a misoperation.

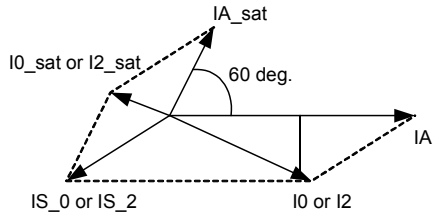

Fig. 26. Principle of sequence phasor rotation

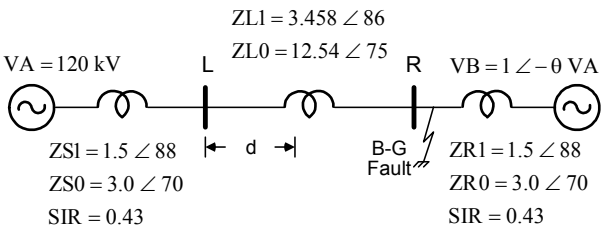

Fig. 27. Elementary network with external phase-B-to-ground fault

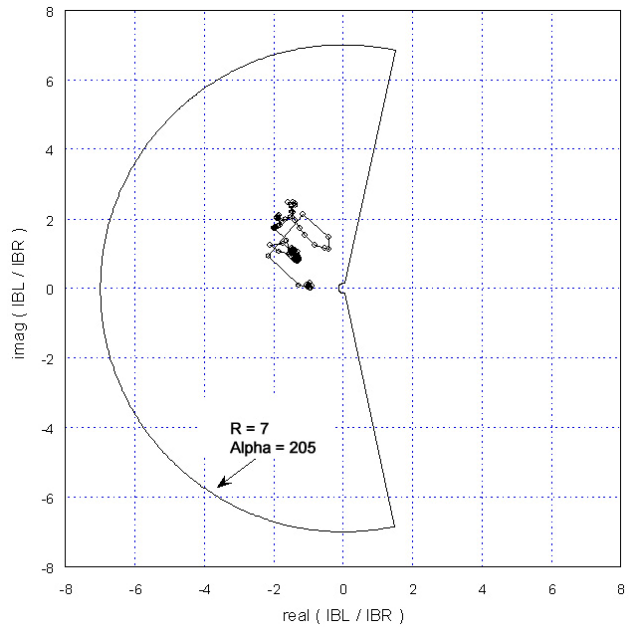

Fig. 28. 87LB current ratio during external fault with saturation

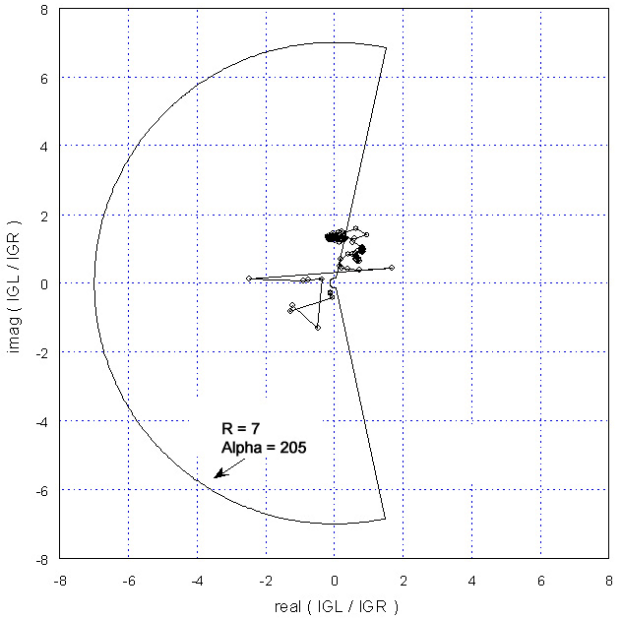

Fig. 29. 87LG current ratio during external fault with saturation

VIII. Conclusions

1. In three-pole tripping applications, sensitivity will be provided by the 87LG and 87L2 sequence elements. The current ratio of these elements will be located entirely in the right-hand side of the complex plane close to the horizontal axis. They are immune to any load effect.
2. In three-pole tripping applications, phase elements (87LA, 87LB, or 87LC) will be subjected to the effect of load and will undergo trajectories that will go inside the stability area at high values of fault resistance or at high values of load angle.
3. In single-pole-tripping applications, subtracting the prefault current (current during the pole open condition) from the fault current will restore the original sensitivity of sequence elements.
4. In all applications, phase element sensitivity equivalent to that achieved with sequence elements can be obtained by removing the prefault current from the fault current. However, it is much simpler to rely on sequence elements for sensitivity provided the prefault current is removed during pole-open situations only.
5. The concept of the saturated current phasor allows for studying the impact of saturation by its introduction in relays steady-state characteristic equations. Because a saturated sequence phasor rotation could be as high as 180 degrees, there is a tendency for both the 87LG and 87L2 elements to become completely unstable and see their trajectory infringe on the right-hand side of the current ratio plane. Misoperation could happen even at moderate levels of saturation. Due to the fact that an 87L0 or 87L2 could become irremediably unstable, they should be blocked when saturation is detected on any of the phase current.
6. A phase characteristic with a large radius R (equal or above 7) and an extended angle alpha (larger than 180 degrees) will be able to sustain high to extreme levels of saturation in phase elements. Immunity to high resistive faults and loading effect will then have to be achieved by sequence elements.
7. In long line applications, careful attention should be exercised so that the pickup level of an element should be above the expected shunt current both in three-pole and single-pole tripping situations.
8. In series-compensated lines applications, a combination of loading effect and current ratio oscillations due to subsynchronous component could make a phase element trajectory infringe into a larger stability characteristic. Pulling back the angle alpha to a value smaller than 180 degrees could be a solution to consider. Special studies should be carried out to determine the nature of the various elements trajectories, and CTs should be properly selected so as to try to avoid saturation.

IX. Appendix A: Resolution of an External Single-Phase-A-to-Ground Fault Using the Sequence Network

For the single-line network of Fig. 30, a single-phase-A-to-ground internal fault at location d from the left bus, L, is resolved using the sequence network of Fig. 31 where the superposition principle is being used. The superposition principle consists in applying to the faulted network (sequence network) a voltage at the fault location equal to the voltage existing at the same point before the fault. The total fault current at some location on the network is equal to the load current existing before the fault plus the pure-fault current (current void of any load) existing on the faulted network.

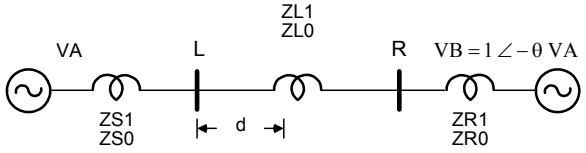

Fig. 30. Single-line network

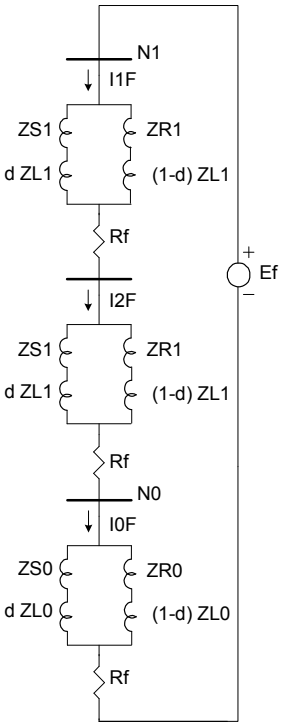

Fig. 31. Phase-A-to-ground fault at R pure-fault sequence network

For the circuit of Fig. 30, the voltage at the fault location prior to the fault is:

$$\mathrm{Ef} = \mathrm{VA} - \mathrm{I_{LD}}\mathrm{Z1M} \tag{28}$$

where Z1M is the impedance between the source VA and the fault location at distance d is:

$$\mathrm{Z1M} = \mathrm{ZS1} + \mathrm{d\ ZL1} \tag{29}$$

The load current in the line is provided by:

$$\mathrm{I_{LD}} = \frac{\left(1 - \mathrm{e}^{-\mathrm{j}\theta}\right)\mathrm{VA}}{\mathrm{Z1M} + \mathrm{Z1N}} \tag{30}$$

where Z1N is defined as:

$$\mathrm{Z1N} = \mathrm{ZR1} + \left(1 - \mathrm{d}\right)\mathrm{ZL1} \tag{31}$$

The total impedance ZSOM in front of the source Ef on the faulted circuit is:

$$\mathrm{ZSOM} = \frac{2\ \mathrm{Z1M}\ \mathrm{Z1N}}{\mathrm{Z1M} + \mathrm{Z1N}} + \frac{\mathrm{Z0M}\ \mathrm{Z0N}}{\mathrm{Z0M} + \mathrm{Z0N}} + 3\ \mathrm{Rf} \tag{32}$$

with Z0M and Z0N being defined as:

$$\mathrm{Z0M} = \mathrm{ZS0} + \mathrm{d\ ZL0} \tag{33}$$

$$\mathrm{Z0N} = \mathrm{ZR0} + \left(1 - \mathrm{d}\right)\mathrm{ZL0} \tag{34}$$

The positive-sequence current at the fault is equal to the source voltage divided by the total impedance:

$$\mathrm{I1F} = \frac{\mathrm{Ef}}{\mathrm{ZSOM}} \tag{35}$$

For a single-phase-A-to-ground fault, the negative- and zero-sequence current at the fault are equal to the positive-sequence current:

$$\mathrm{I2F} = \mathrm{I1F} \tag{36}$$

$$\mathrm{I0F} = \mathrm{I1F} \tag{37}$$

The positive-, negative-, and zero-sequence currents at the relay location close to the L bus are provided as:

$$\mathrm{I1L} = \mathrm{C1\ I1F} \tag{38}$$

$$\mathrm{I2L} = \mathrm{C1\ I1F} \tag{39}$$

$$\mathrm{I0L} = \mathrm{C0\ I1F} \tag{40}$$

where C1 and C0 are the current distribution factors at the relay location and are equal to:

$$\mathrm{C1} = \frac{\mathrm{Z1N}}{\mathrm{Z1M} + \mathrm{Z1N}} \tag{41}$$

$$\mathrm{C0} = \frac{\mathrm{Z0N}}{\mathrm{Z0M} + \mathrm{Z0N}} \tag{42}$$

The positive-, negative-, and zero-sequence currents at the relay location close to the R bus are provided as:

$$\mathrm{I1R} = \left(1 - \mathrm{C1}\right)\mathrm{I1F} \tag{43}$$

$$\mathrm{I2R} = \left(1 - \mathrm{C1}\right)\mathrm{I1F} \tag{44}$$

$$\mathrm{I0R} = \left(1 - \mathrm{C0}\right)\mathrm{I1F} \tag{45}$$

The phase-A current at the relay location close to the L bus is:

$$\begin{aligned}\mathrm{IAL} &= \mathrm{C1\ I1F} + \mathrm{C2\ I2F} + \mathrm{C0\ I0F} + \mathrm{I_{LD}} \\ &= \left(2\ \mathrm{C1} + \mathrm{C0}\right)\mathrm{I1F} + \mathrm{I_{LD}}\end{aligned} \tag{46}$$

The phase-A current at the relay close to the R bus is:

$$\mathrm{IAR} = \left[2\left(1 - \mathrm{C1}\right) + \left(1 - \mathrm{C0}\right)\right]\mathrm{I1F} - \mathrm{I_{LD}} \tag{47}$$

X. Appendix B: Resolution of an Internal Single-Phase-A-To-Ground Fault With Phase-B Open Using the Sequence Network

Consider the elementary network of Fig. 30; the sequence network corresponding to a phase-B open situation is represented in Fig. 32.

In order to draw the sequence network for a phase-B open situation, two constraints must be embedded into the network: a voltage constraint and a current constraint. Assume that phase-B is open between two points, x and y. Obviously, the sequence voltages between points x and y are provided by the following conditions:

$$\begin{pmatrix} \mathrm{V1_{xy}} \\ \mathrm{V2_{xy}} \\ \mathrm{V0_{xy}} \end{pmatrix} = \frac{1}{3} \cdot \begin{pmatrix} 1 & \mathrm{a} & \mathrm{a}^2 \\ 1 & \mathrm{a}^2 & \mathrm{a} \\ 1 & 1 & 1 \end{pmatrix} \cdot \begin{pmatrix} \mathrm{VA_{xy}} \\ \mathrm{VB_{xy}} \\ \mathrm{VC_{xy}} \end{pmatrix} \tag{48}$$

In (48), "a" is the conventional complex operator $1\angle 120°$. Obviously, $\mathrm{VA_{xy}}$ and $\mathrm{VC_{xy}}$ are zero so that we end up with:

$$\begin{aligned}\mathrm{V1_{xy}} &= \left(1/3\right)\mathrm{a\ VB_{xy}} \\ \mathrm{V2_{xy}} &= \left(1/3\right)\mathrm{a}^2\ \mathrm{VB_{xy}} \\ \mathrm{V0_{xy}} &= \left(1/3\right)\mathrm{VB_{xy}}\end{aligned} \tag{49}$$

Regarding the current constraint, it is expressed by the condition that the phase-B current must be equal to zero or:

$$\mathrm{IB} = \mathrm{a}^2\ \mathrm{I1L} + \mathrm{a\ I2L} + \mathrm{I0L} = 0 \tag{50}$$

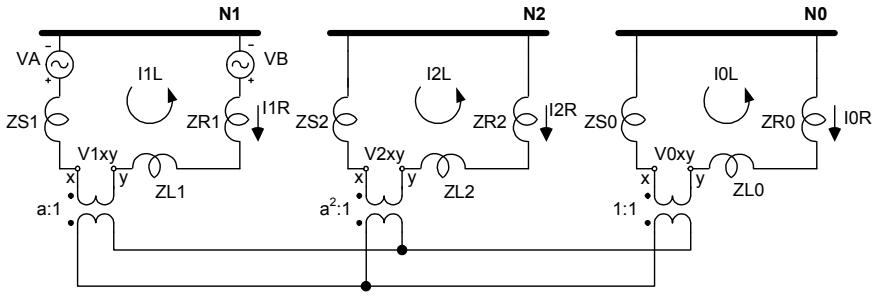

Fig. 32. Sequence network of phase-B open elementary network

$$\begin{pmatrix} ZL1+ZS1+ZR1 & 0 & 0 & a \\ 0 & ZL1+ZS1+ZR1 & 0 & a^2 \\ 0 & 0 & ZL0+ZS0+ZR0 & 1 \\ a^2 & a & 1 & 0 \end{pmatrix} \cdot \begin{pmatrix} I1L \\ I2L \\ I0L \\ (1/3)VB_{xy} \end{pmatrix} = \begin{pmatrix} VA-VB \\ 0 \\ 0 \\ 0 \end{pmatrix} \tag{51}$$

The three ideal transformers represented in the sequence network of Fig. 32 implement the two voltage and current constraints.

The sequence network of Fig. 32 can be resolved for the unknown sequence currents by solving the (51) linear matrix equation.

Let us define the following variables:

$$\begin{aligned} \Delta V &= VA - VB \\ m &= ZL1+ZS1+ZR1 = ZL2+ZS2+ZR2 \\ n &= ZL0+ZS0+ZR0 \\ m_1 &= -(1-d)\,ZL1 - ZR1 \\ n_1 &= -(1-d)\,ZL0 - ZR0 \\ p &= m + m_1 = d\,ZL1 + ZS1 = d\,ZL2 + ZS2 \\ q &= n + n_1 = d\,ZL0 + ZS0 = d\,ZL0 + ZS0 \end{aligned} \tag{52}$$

Using the Gaussian elimination process can resolve the system of equations in (51) and leads to the solution for the three sequence currents as:

$$I1L_{preflt} = -I1R_{preflt} = \frac{\Delta V\,(m+n)}{m\,(m+2\,n)} \tag{53}$$

$$I2L_{preflt} = -I2R_{preflt} = -\frac{a\,\Delta V\,n}{m\,(m+2\,n)} \tag{54}$$

$$I0L_{preflt} = -I0R_{preflt} = -\frac{a^2\,\Delta V}{m+2\,n} \tag{55}$$

It should be borne in mind at this stage of the analysis that the three sequence currents determined during the phase-B open condition constitute the prefault currents before any other fault would occur at a later stage. For this reason, the sequence currents have been shown in (53) through (55) with a prefault subscript.

Following the same reasoning, the phase-A prefault current on the left side can be computed as the sum of all three sequence currents:

$$IAL_{preflt} = \frac{m\,\Delta V\,(1-a^2) + n\,\Delta V\,(1-a)}{m\,(m+2\,n)} \tag{56}$$

The phase-A current on the right side is the opposite of the former as:

$$IAR_{preflt} = -\frac{m\,\Delta V\,(1-a^2) + n\,\Delta V\,(1-a)}{m\,(m+2\,n)} \tag{57}$$

Let us assume now that during the open phase-B condition, a subsequent phase-A-to-ground fault occurs at a distance, d, from the left bus of the line. This faulted sequence network is represented in Fig. 33, where the new condition of a phase-A-to-G has been added to the already represented pole-open B condition. The sequence currents can now be resolved by solving the next set of linear equations:

$$\begin{pmatrix} ZL1+ZS1+ZR1 & 0 & 0 & -(1-d)\,ZL1-ZR1 & a \\ 0 & ZL2+ZS2+ZR2 & 0 & -(1-d)\,ZL2-ZR2 & a^2 \\ 0 & 0 & ZL0+ZS0+ZR0 & -(1-d)\,ZL0-ZR0 & 1 \\ ZS1+d\,ZL1 & ZS2+d\,ZL2 & ZS0+d\,ZL0 & 3R & 0 \\ a^2 & a & 1 & 0 & 0 \end{pmatrix} \begin{pmatrix} I1L \\ I2L \\ I0L \\ IF \\ (1/3)VB_{xy} \end{pmatrix} = \begin{pmatrix} \Delta V \\ 0 \\ 0 \\ VA \\ 0 \end{pmatrix} \tag{58}$$

By using the same Gaussian elimination process as before, the current at the fault IF and the sequence currents at the left-hand-side line bus can be computed as:

$$IF = \frac{-2\,a^2\,m\,\Delta V\,(-0.5\,p-q) - \Delta V\,p\,(1-a)(m+2\,n) + 2\,m\,VA\,(m+2\,n)}{2\,m\,(-0.5\,p-q)(m_1+2\,n_1) - 3\,p\,m_1\,(m+2\,n) + 6\,R_f\,m\,(m+2\,n)} \tag{59}$$

$$I0L = \frac{-a^2\,\Delta V}{m+2n} - \frac{m_1+2n_1}{m+2n}\,IF \tag{60}$$

$$I2L = \frac{-a\,\Delta V\,n}{m(m+2n)} + \left(\frac{a^2}{2}\,\frac{m_1+2n_1}{m+2n} - \frac{m_1(1-a)}{2m}\right)IF \tag{61}$$

$$I1L = \frac{\Delta V(m+n)}{m(m+2n)} + \left(\frac{a}{2}\,\frac{m_1+2n_1}{m+2n} + \frac{m_1(a^2-1)}{2m}\right)IF \tag{62}$$

The phase-A fault current on the left side is equal to the sum of the three sequence currents:

$$IAL = \frac{\Delta V(m+n)}{m(m+2n)} + \frac{-a\,\Delta V\,n}{m(m+2n)} - \frac{a^2\,\Delta V}{m+2n} + \left(\left(\frac{a^2}{2}+\frac{a}{2}-1\right)\left(\frac{m_1+2n_1}{m+2n}\right) + \frac{m_1(a^2-2+a)}{2m}\right)IF \tag{63}$$

The sequence currents at the right-hand-side bus can be computed as:

$$I0R = \frac{a^2\,\Delta V}{m+2n} + \frac{p+2q}{m+2n}\,IF \tag{64}$$

$$I2R = \frac{a\,\Delta V\,n}{m(m+2n)} + \left(1 - \frac{a^2}{2}\,\frac{m_1+2n_1}{m+2n} + \frac{m_1(1-a)}{2m}\right)IF \tag{65}$$

$$I1R = -\frac{\Delta V(m+n)}{m(m+2n)} + \left(1 - \frac{a}{2}\,\frac{m_1+2n_1}{m+2n} - \frac{m_1(a^2-1)}{2m}\right)IF \tag{66}$$

The phase-A fault current on the right-hand side is equal to the sum of the three sequence currents:

$$IAR = \frac{\Delta V(m+n)}{m(m+2n)} + \frac{a\,\Delta V\,n}{m(m+2n)} + \frac{a^2\,\Delta V}{m+2n} + \begin{pmatrix} 2 + \dfrac{p+2q-\left(\dfrac{a^2}{2}+\dfrac{a}{2}\right)(m_1+2n_1)}{m+2n} \\ -\dfrac{m_1(a^2-2+a)}{2m} \end{pmatrix} IF \tag{67}$$

Looking at (60) through (62) for the left-hand-side bus and (64) through (66) for the right-hand-side bus and considering (53) through (55) for the sequence currents in the open-pole situation only, notice that the sequence currents at both extremities of the lines are composed of a prefault term and a second term that is proportional to IF, so that we can now write:

$$I0L = I0L_{preflt} - \frac{m_1+2n_1}{m+2n}\,IF \tag{68}$$

$$I2L = I2L_{preflt} + \left(\frac{a^2}{2}\,\frac{m_1+2n_1}{m+2n} - \frac{m_1(1-a)}{2m}\right)IF \tag{69}$$

$$I1L = I1L_{preflt} + \left(\frac{a}{2}\,\frac{m_1+2n_1}{m+2n} + \frac{m_1(a^2-1)}{2m}\right)IF \tag{70}$$

$$I0R = I0R_{preflt} + \frac{p+2q}{m+2n}\,IF \tag{71}$$

$$I2R = I2R_{preflt} + \left(1 - \frac{a^2}{2}\,\frac{m_1+2n_1}{m+2n} + \frac{m_1(1-a)}{2m}\right)IF \tag{72}$$

$$I1R = I1R_{preflt} + \left(1 - \frac{a}{2}\,\frac{m_1+2n_1}{m+2n} - \frac{m_1(a^2-1)}{2m}\right)IF \tag{73}$$

Following the same line of thinking, the two phase-A currents in (63) and (67) are at both extremities of the line and can be expressed as:

$$IAL = IAL_{preflt} + \left(\left(\frac{a^2}{2}+\frac{a}{2}-1\right)\left(\frac{m_1+2n_1}{m+2n}\right) + \frac{m_1(a^2-2+a)}{2m}\right)IF \tag{74}$$

and:

$$IAR = IAR_{preflt} + \begin{pmatrix} 2 + \dfrac{p+2q-\left(\dfrac{a^2}{2}+\dfrac{a}{2}\right)(m_1+2n_1)}{m+2n} \\ -\dfrac{m_1(a^2-2+a)}{2m} \end{pmatrix} IF \tag{75}$$

Following the next identity:

$$a^2 + a = -1 \tag{76}$$

Equations (74) and (75) can be rewritten as:

$$IAL = IAL_{preflt} - \frac{3}{2}\left(\frac{m_1+2n_1}{m+2n} + \frac{m_1}{m}\right)IF \tag{77}$$

$$IAR = IAR_{preflt} + \left(2 + \frac{p+2q-0.5(m_1+2n_1)}{m+2n} + \frac{3m_1}{2m}\right)IF \tag{78}$$

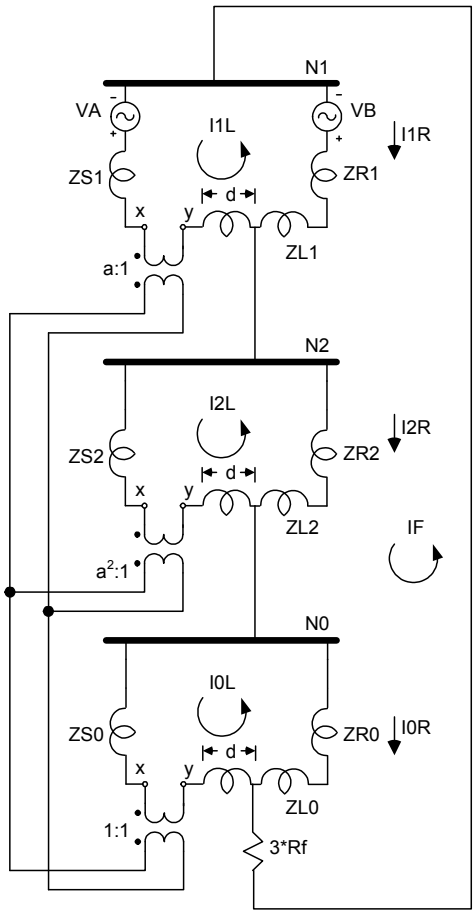

Fig. 33. Sequence network of phase-B open with phase-A-to-ground fault elementary network

Looking at (68) through (73) providing the sequence currents at both extremities of the line and at (77) and (78) providing the phase-A currents, one can see that any current can be expressed in the general form corresponding to:

$$I = I_{preflt} + \text{func}\left(d, ZSl, ZL1, ZR1, ZS0, ZL0, ZR0\right) IF \quad (79)$$

In (79), any current, phase, or sequence can be expressed as the sum of the current existing before the fault and the product of a function "func" by the current IF flowing into the fault in the sequence network. The function "func," in turn, is a function of the distance to the fault and the network impedances only.

The current IF flowing into the fault is a function of the distance to the fault, the network impedances, the source voltages, and, most important of all, the fault resistance Rf.

$$IF = \text{func}\left(d, ZSl, ZL1, ZR1, ZS0, ZL0, ZR0, Rf, VA, VB\right) \quad (80)$$

XI. References

[1] J. Roberts, D. Tziouvaras, G. Benmouyal, and H. Altuve, "The Effect of Multiprinciple Line Protection on Dependability and Security," proceedings of the 55th Annual Georgia Tech Protective Relaying Conference, Atlanta, GA, May 2001.

[2] G. Benmouyal and T. Lee, "Securing Sequence Current Differential Elements," proceedings of the 31st Annual Western Protective Relay Conference, Spokane, WA, October 2004.

[3] F. Calero and D. Hou, "Practical Single-Pole Line Protection Scheme Considerations," proceedings of the 31st Annual Western Protective Relay Conference, Spokane, WA, October 2004.

[4] L. J. Ernst, W. L. Hinman, D. H. Quam, and J. S. Thorp, "Charge Comparison Protection of Transmission Lines – Relaying Concepts," *IEEE Transactions on Power Delivery*, Vol. 7, Nº 4, October 1992, pp. 1834–1852.

[5] J. Roberts, T. J. Lee, and G. E. Alexander, "Security and Dependability of Multiterminal Transmission Line Protection," proceedings of the 28th Annual Western Protective Relay Conference, Spokane, WA, October 2001.

[6] A. R. van C. Warrington, *Protective Relays: Their Theory and Practice,* Volume One, London: Chapman and Hall, 1962.

[7] A. R. van C. Warrington, *Protective Relays: Their Theory and Practice,* Volume Two*,* London: Chapman and Hall, 1969.

[8] S. E. Zocholl, "Rating CTs for Low-Impedance Bus and Machine Differential Applications," proceedings of the 27th Annual Western Protective Relay Conference, Spokane, WA, October 2000.

[9] G. Benmouyal and S. E. Zocholl, "Impact of High Fault Current and CT Rating Limits on Overcurrent Protection," proceedings of the 29th Annual Western Protective Relay Conference, Spokane, WA, October 2002.

[10] S. E. Zocholl, G. Benmouyal, and J. Roberts, "Selecting CTs to Optimize Relay Performance," 23rd Annual Western Protective Relay Conference, Spokane, WA, October 1996.

[11] S. E. Zocholl and D. W. Smaha, "Current Transformer Concepts," proceedings of the 46th Annual Georgia Tech Protective Relay Conference, Atlanta, GA, April 1992.

XII. Biography

Gabriel Benmouyal, P.E. received his B.A.Sc. in Electrical Engineering and his M.A.Sc. in Control Engineering from Ecole Polytechnique, Université de Montréal, Canada, in 1968 and 1970, respectively. In 1969, he joined Hydro-Québec as an Instrumentation and Control Specialist. He worked on different projects in the field of substation control systems and dispatching centers. In 1978, he joined IREQ, where his main field of activity has been the application of microprocessors and digital techniques for substation and generating-station control and protection systems. In 1997, he joined Schweitzer Engineering Laboratories, Inc. in the position of Principal Research Engineer. He is a registered professional engineer in the Province of Québec, is an IEEE Senior Member, and has served on the Power System Relaying Committee since May 1989. He holds over six patents and is the author or co-author of several papers in the field of signal processing and power networks protection.